Rotating black holes with Dehnen dark matter halo

Supakchai Ponglertsakul

Based on 2608.05861 [gr-qc]: with: David Senjaya

17 August 2026, SHEAP

Plan

Galaxy rotation's curve

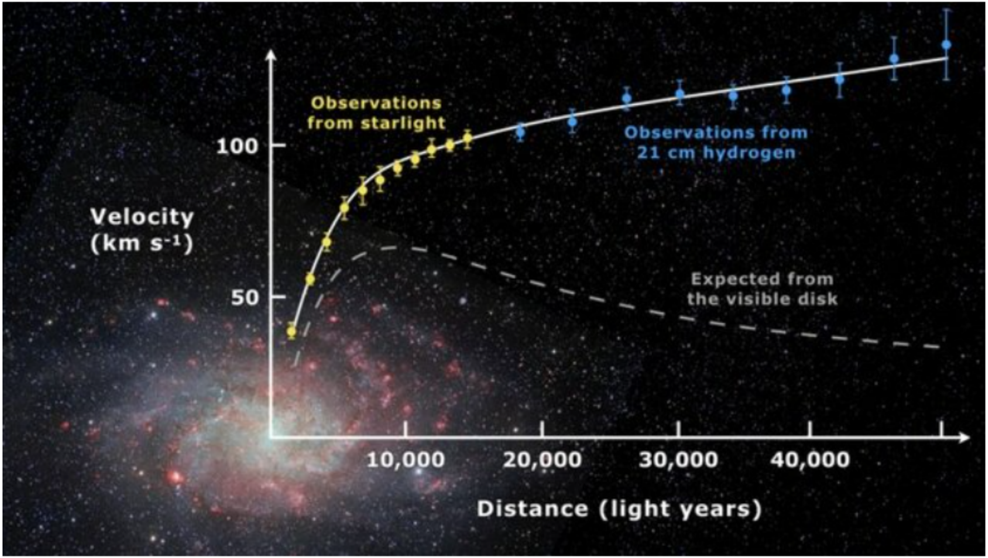

Bullet cluster

Figure: NASA's Chandra-Observatory

Bullet cluster

Cr: CAASTO

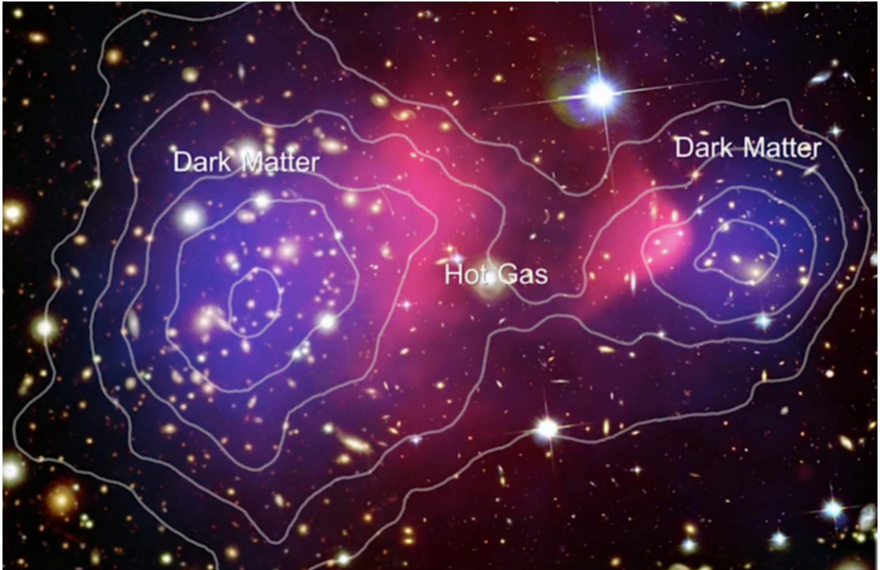

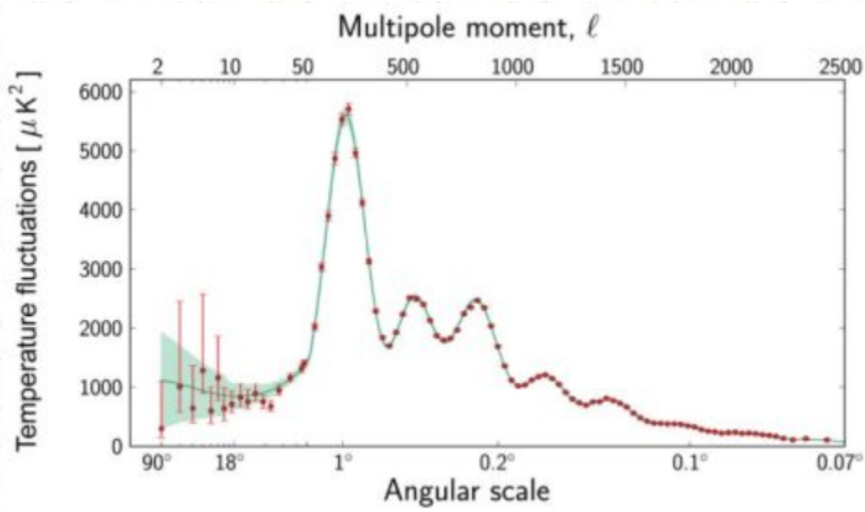

Figure: Planck

DM properties[1]

- Massive
- Dark, i.e., electrically neutral
- Weakly interact with normal matter
- Cold*, slow-moving
- Stable on cosmic scale

[1] Credit: Patipan's talk @WE-Heraeus

DM properties[1]

Cr: TikZ.net

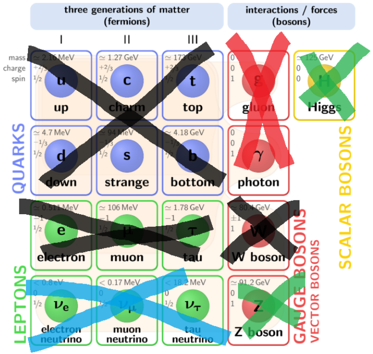

- Massive
- Dark, i.e., electrically neutral
- Weakly interact with normal matter
- Cold*, slow-moving
- Stable on cosmic scale

None of these matches any (known) Standard Model particles.

[1] Credit: Patipan's talk @WE-Heraeus

Cold vs Warm DM

Cold DM

- Large-scale structure: well explained
- Missing satellite problem: predicts (more) dwarf galaxies orbiting large galaxies.
- Core-cusp problem: predicts a sharp spike at the galactic center (a cusp).

Warm DM

- Solve the core-cusp problem
- Matches large scale structure
- Slower-clumping matter predicts first stars and galaxies formed much later than in the CDM Model.

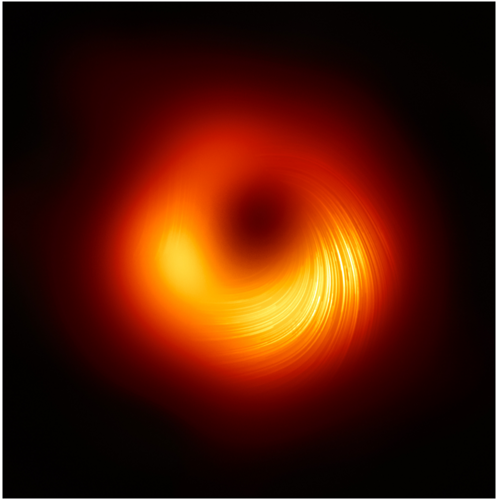
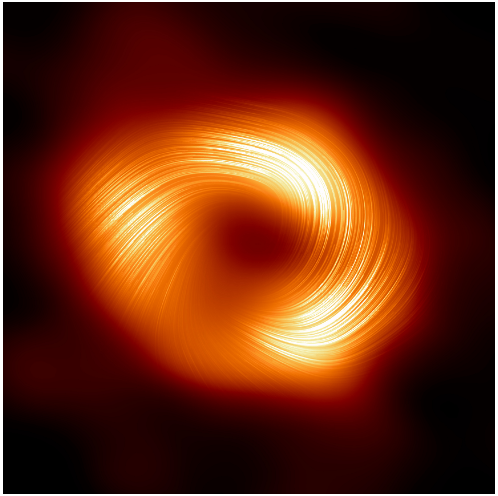

Figure: EHT collaboration

Black holes and dark matter

- They must co-exist.
- Although dark matter does not emit light, it can still be accreted by black holes.
- DM influences the growth of black holes and the evolution of galaxies.

Question

How do we model a dark matter halo?

Black holes and dark matter

- They must co-exist.
- Although dark matter does not emit light, it can still be accreted by black holes.
- DM influences the growth of black holes and the evolution of galaxies.

Question

How do we model a dark matter halo?

Answer

- By constructing its "density profile", usually depends on characteristic density and some length scale.
- It tells us how dark matter is generally distributed around the galactic center.

Navarro-Frenk-White profile[3]

- Found by large-N bodies simulation of *cold dark matter*.

[2] Gondolo and Silk, Phys.Rev.Lett. 83 (1999) 1719-1722
[3] Astrophys.J.462:563-575,1996

Navarro-Frenk-White profile[3]

- Found by large-N bodies simulation of *cold dark matter*.
- It predicts a highly concentrated DM density at the center, i.e., a cusp profile..

[2] Gondolo and Silk, Phys.Rev.Lett. 83 (1999) 1719-1722
[3] Astrophys.J.462:563-575,1996

Navarro-Frenk-White profile[3]

- Found by large-N bodies simulation of *cold dark matter*.
- It predicts a highly concentrated DM density at the center, i.e., a cusp profile..
- Observations suggests rather a constant density central region or *cored profile*.

[2] Gondolo and Silk, Phys.Rev.Lett. 83 (1999) 1719-1722
[3] Astrophys.J.462:563-575,1996

Navarro-Frenk-White profile[3]

- Found by large-N bodies simulation of *cold dark matter*.
- It predicts a highly concentrated DM density at the center, i.e., a cusp profile..
- Observations suggests rather a constant density central region or *cored profile*.
- With SMBH, it is worse. The BH redistributes the density profile, creating a *spike*[2].

[2] Gondolo and Silk, Phys.Rev.Lett. 83 (1999) 1719-1722
[3] Astrophys.J.462:563-575,1996

Navarro-Frenk-White profile[3]

- Found by large-N bodies simulation of *cold dark matter*.
- It predicts a highly concentrated DM density at the center, i.e., a cusp profile..
- Observations suggests rather a constant density central region or *cored profile*.
- With SMBH, it is worse. The BH redistributes the density profile, creating a *spike*[2].

The spike

- This significantly increases the density in the central region. More DM is drawn toward the BH.

[2] Gondolo and Silk, Phys.Rev.Lett. 83 (1999) 1719-1722

[3] Astrophys.J.462:563-575,1996

Navarro-Frenk-White profile[3]

- Found by large-N bodies simulation of *cold dark matter*.
- It predicts a highly concentrated DM density at the center, i.e., a cusp profile..
- Observations suggests rather a constant density central region or *cored profile*.
- With SMBH, it is worse. The BH redistributes the density profile, creating a *spike*[2].

The spike

- This significantly increases the density in the central region. More DM is drawn toward the BH.
- DM annihilation rate (if exists) is extremely increased. Thus, end-product particles such as neutrinos should be observed at the galactic center.

[2] Gondolo and Silk, Phys.Rev.Lett. 83 (1999) 1719-1722
[3] Astrophys.J.462:563-575,1996

Navarro-Frenk-White profile[3]

- Found by large-N bodies simulation of *cold dark matter*.
- It predicts a highly concentrated DM density at the center, i.e., a cusp profile..
- Observations suggests rather a constant density central region or *cored profile*.
- With SMBH, it is worse. The BH redistributes the density profile, creating a *spike*[2].

The spike

- This significantly increases the density in the central region. More DM is drawn toward the BH.
- DM annihilation rate (if exists) is extremely increased. Thus, end-product particles such as neutrinos should be observed at the galactic center.
- Mass of DM spike should alter stellar orbit around the center.

[2] Gondolo and Silk, Phys.Rev.Lett. 83 (1999) 1719-1722
[3] Astrophys.J.462:563-575,1996

Other profiles

Double power law

$$\rho(r) = \rho_0 \left(\frac{r}{r_0}\right)^{-\gamma} \left[1 + \left(\frac{r}{r_0}\right)^{\alpha}\right]^{(\gamma-\beta)/\alpha}.$$

Other profiles

Double power law

$$\rho(r) = \rho_0 \left(\frac{r}{r_0}\right)^{-\gamma} \left[1 + \left(\frac{r}{r_0}\right)^{\alpha}\right]^{(\gamma-\beta)/\alpha} .$$

Cored

- Pseudo isothermal
- Burkert $(2, 3, 1)$
- Perfect sphere $(2, 4, 0)$
- Plummer sphere $(2, 5, 0)$

Cuspy

- NFW $(1, 3, 1)$
- Einasto
- Hernquist $(1, 4, 1)$
- Jaffe $(1, 4, 2)$
- Dehnen $(1, 4, \gamma)$

What and Why Dehnen[4]?

Double power law

$$\rho(r) = \rho_0 \left(\frac{r}{r_0}\right)^{-\gamma} \left[1 + \frac{r}{r_0}\right]^{(\gamma-4)} .$$

$$M(r) = 4\pi \int_0^r \rho(r') r'^2 dr' \propto \frac{1}{(\gamma - 3)}.$$

- $\rho \sim r^{-4}, r \to \infty$ and $\rho \sim r^{-\gamma}, r \to 0$: Thus $\gamma = 0$ gives a cored profile.

[4] W. Dehnen, Mon. Not. r. Astron. Soc. 265,250-256 (1993)

What and Why Dehnen[4]?

Double power law

$$\rho(r) = \rho_0 \left(\frac{r}{r_0}\right)^{-\gamma} \left[1 + \frac{r}{r_0}\right]^{(\gamma-4)} .$$

$$M(r) = 4\pi \int_0^r \rho(r')r'^2 dr' \propto \frac{1}{(\gamma-3)}.$$

- $\rho \sim r^{-4}, r \to \infty$ and $\rho \sim r^{-\gamma}, r \to 0$: Thus $\gamma = 0$ gives a cored profile.
- Only $0 \leq \gamma < 3$ gives physical DM mass profile.

[4] W. Dehnen, Mon. Not. r. Astron. Soc. 265,250-256 (1993)

What and Why Dehnen[4]?

Double power law

$$\rho(r) = \rho_0 \left(\frac{r}{r_0}\right)^{-\gamma} \left[1 + \frac{r}{r_0}\right]^{(\gamma-4)} .$$

$$M(r) = 4\pi \int_0^r \rho(r')r'^2 dr' \propto \frac{1}{(\gamma-3)}.$$

- $\rho \sim r^{-4}, r \to \infty$ and $\rho \sim r^{-\gamma}, r \to 0$: Thus $\gamma = 0$ gives a cored profile.
- Only $0 \leq \gamma < 3$ gives physical DM mass profile.
- It is flexible and can give rise to various profiles, whether cuspy or cored.

[4] W. Dehnen, Mon. Not. r. Astron. Soc. 265,250-256 (1993)

What and Why Dehnen[4]?

Double power law

$$\rho(r) = \rho_0 \left(\frac{r}{r_0}\right)^{-\gamma} \left[1 + \frac{r}{r_0}\right]^{(\gamma-4)} .$$

$$M(r) = 4\pi \int_0^r \rho(r') r'^2 dr' \propto \frac{1}{(\gamma - 3)}.$$

- $\rho \sim r^{-4}, r \to \infty$ and $\rho \sim r^{-\gamma}, r \to 0$: Thus $\gamma = 0$ gives a cored profile.
- Only $0 \leq \gamma < 3$ gives physical DM mass profile.
- It is flexible and can give rise to various profiles, whether cuspy or cored.
- It was originally developed to describe light distribution in galaxies i.e., stellar (mass) distribution.

[4] W. Dehnen, Mon. Not. r. Astron. Soc. 265,250-256 (1993)

What and Why Dehnen[4]?

Double power law

$$\rho(r) = \rho_0 \left(\frac{r}{r_0}\right)^{-\gamma} \left[1 + \frac{r}{r_0}\right]^{(\gamma-4)} .$$

$$M(r) = 4\pi \int_0^r \rho(r')r'^2 dr' \propto \frac{1}{(\gamma - 3)}.$$

- $\rho \sim r^{-4}, r \to \infty$ and $\rho \sim r^{-\gamma}, r \to 0$: Thus $\gamma = 0$ gives a cored profile.
- Only $0 \leq \gamma < 3$ gives physical DM mass profile.
- It is flexible and can give rise to various profiles, whether cuspy or cored.
- It was originally developed to describe light distribution in galaxies i.e., stellar (mass) distribution.
- Its flexibility has proven useful when modeling cuspy or cored DM profiles.

[4] W. Dehnen, Mon. Not. r. Astron. Soc. 265,250-256 (1993)

What and Why Dehnen?

- For dwarf galaxies, cuspy/cored DM profile is *debatable*.

[5] BH with Dehnen DM profile is explored in JCAP 08, 056 (2022).

What and Why Dehnen?

- For dwarf galaxies, cuspy/cored DM profile is *debatable*.
- The dynamical friction of the stellar distribution requires more precise observations.

[5] BH with Dehnen DM profile is explored in JCAP 08, 056 (2022).

What and Why Dehnen?

- For dwarf galaxies, cuspy/cored DM profile is *debatable*.
- The dynamical friction of the stellar distribution requires more precise observations.
- Dwarf galaxies cannot host supermassive black holes. Recent observations suggest otherwise.

[5] BH with Dehnen DM profile is explored in JCAP 08, 056 (2022).

What and Why Dehnen?

- For dwarf galaxies, cuspy/cored DM profile is *debatable*.
- The dynamical friction of the stellar distribution requires more precise observations.
- Dwarf galaxies cannot host supermassive black holes. Recent observations suggest otherwise.
- Dwarf galaxies: Mrk 462, Henize 2-10, Leo I host SMBH, $M \sim 2 \times 10^5 M_\odot, 1 \times 10^6 M_\odot, 3.3 \times 10^6 M_\odot$.

[5] BH with Dehnen DM profile is explored in JCAP 08, 056 (2022).

What and Why Dehnen?

- For dwarf galaxies, cuspy/cored DM profile is *debatable*.
- The dynamical friction of the stellar distribution requires more precise observations.
- Dwarf galaxies cannot host supermassive black holes. Recent observations suggest otherwise.
- Dwarf galaxies: Mrk 462, Henize 2-10, Leo I host SMBH, $M \sim 2 \times 10^5 M_\odot, 1 \times 10^6 M_\odot, 3.3 \times 10^6 M_\odot$.
- Ultra-faint dwarf galaxies ($r \sim 98 ly, L = 10^{2-3} L_\odot$) $\rightarrow$ highest halo-mass to baryon-mass ratio, thus the most dark matter dominated system $\rightarrow$ a good laboratory to explore DM[5]

[5] BH with Dehnen DM profile is explored in JCAP 08, 056 (2022).

What and Why?

- Burkert *1905.11803*
- Navarro-Frenk-White *2303.08183*
- Hernquist $(1, 4, 1)$ *2303.17666*
- Einasto: $\rho = \rho_0 e^{-2\alpha^{-1}((r/r_0)^{\alpha}-1)}$ *2307.13553*

What and Why?

- Burkert *1905.11803*
- Navarro-Frenk-White *2303.08183*
- Hernquist $(1,4,1)$ *2303.17666*
- Einasto: $\rho = \rho_0 e^{-2\alpha^{-1}((r/r_0)^{\alpha}-1)}$ *2307.13553*
- Dehnen $(1,4,0),(1,4,1/2),(1,4,3/2),(1,4,5/2)$ *2407.0287,2411.01145,2602.03349*
- Jaffe $(1,4,2)$ *2505.20031*
- Several static/rotating BH solutions including regular black holes are found with various DM profiles.

Objective

Construct static and rotating black holes with double power law profile. Compute quasi-boundstate and amplification factor of energy extraction process of rotating black hole.

Static solution

- General static spherically symmetric ansatz

$$ds^2 = -f(r)\, dt^2 + \frac{dr^2}{f(r)} + r^2 \left(d\theta^2 + \sin^2\theta \, d\phi^2\right) , \tag{1}$$

- We model the dark matter halo as an anisotropic fluid with energy–momentum tensor

$$T^{\mu}_{\ \nu} = \mathrm{diag}\left[-\rho_{\mathrm{DM}}(r),\ p_r(r),\ p_t(r),\ p_t(r)\right] ,$$

Static solution

- General static spherically symmetric ansatz

$$ds^2 = -f(r)\,dt^2 + \frac{dr^2}{f(r)} + r^2\left(d\theta^2 + \sin^2\theta\,d\phi^2\right), \tag{1}$$

- We model the dark matter halo as an anisotropic fluid with energy–momentum tensor

$$T^{\mu}_{\ \nu} = \mathrm{diag}\left[-\rho_{\mathrm{DM}}(r),\, p_r(r),\, p_t(r),\, p_t(r)\right], \tag{2}$$

- The Einstein field equations $G^{\mu}_{\ \nu} = 8\pi T^{\mu}_{\ \nu}$ yield

$$\left.\begin{aligned} G^{t}_{\ t} &= \frac{1}{r^2}\left[rf'(r) + f(r) - 1\right] = -8\pi\rho_{\mathrm{DM}}(r), && (3)\\ G^{r}_{\ r} &= \frac{1}{r^2}\left[rf'(r) + f(r) - 1\right] = 8\pi p_r(r), && (4)\end{aligned}\right\}\ \rho_{DM} = -p_r$$

$$G^{\theta}_{\ \theta} = \frac{1}{2}f''(r) + \frac{1}{r}f'(r) = 8\pi p_t(r). \tag{5}$$

Static solution

- Temporal component of the Einstein equation gives

$$\frac{d}{dr}\left[r\left(1-f(r)\right)\right] = 8\pi r^2 \rho_{\mathrm{DM}}(r), \tag{6}$$

- Here we insert double power law profile

$$\rho_{\mathrm{DM}}(r) = \rho_0 \left(\frac{r}{r_0}\right)^{-\gamma} \left(1 + \left(\frac{r}{r_0}\right)^{\alpha}\right)^{\frac{\gamma-\beta}{\alpha}}, \tag{7}$$

where ρ_0 and r_0 are the characteristic density and scale radius, respectively. The parameters α, β, γ determine the shape of density profile.

Static solution

Static spherically symmetric solution

$$f(r) = 1 - \frac{r_s}{r} - \frac{8\pi\rho_0 r_0^{\gamma}}{3-\gamma}\, r^{2-\gamma}\, {}_2F_1\left(\frac{3-\gamma}{\alpha}, \frac{\beta-\gamma}{\alpha}; 1 + \frac{3-\gamma}{\alpha}; -\left(\frac{r}{r_0}\right)^{\alpha}\right), \tag{8}$$

- $r_s \equiv 2M, f \to Schwarzschild, \rho_0 \to 0.$

Static solution

Static spherically symmetric solution

$$f(r) = 1 - \frac{r_s}{r} - \frac{8\pi\rho_0 r_0^{\gamma}}{3-\gamma}\, r^{2-\gamma}\, {}_2F_1\left(\frac{3-\gamma}{\alpha}, \frac{\beta-\gamma}{\alpha}; 1+\frac{3-\gamma}{\alpha}; -\left(\frac{r}{r_0}\right)^{\alpha}\right), \tag{8}$$

- $r_s \equiv 2M, f \to Schwarzschild, \rho_0 \to 0.$
- The radial p_r and tangential pressure p_t are

$$p_r = -\rho_0 \left(\frac{r}{r_0}\right)^{-\gamma} \left(1+\left(\frac{r}{r_0}\right)^{\alpha}\right)^{\frac{\gamma-\beta}{\alpha}}, \tag{9}$$

$$p_t = \frac{\rho_0}{2} \left(\frac{r}{r_0}\right)^{-\gamma} \left(1+\left(\frac{r}{r_0}\right)^{\alpha}\right)^{-\frac{\alpha+\beta-\gamma}{\alpha}} \left[(\gamma-2)-(\beta-2)\left(\frac{r}{r_0}\right)^{\alpha}\right]. \tag{10}$$

Static solution

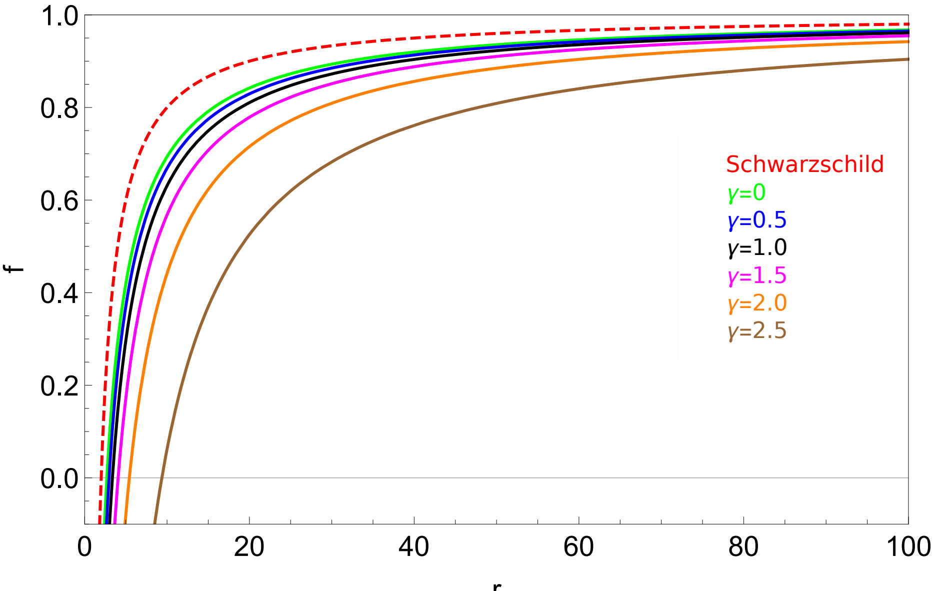

Static solution

- Dehnen $(1,4,0)$:

$$\lim_{r\to 0}\{R, R^2, K\} \to \left\{32\pi\rho_0 - \mathcal{O}(r), 256\pi^2\rho_0^2 - \mathcal{O}(r), \frac{48M^2}{r^6} - \mathcal{O}(\frac{\rho_0}{r^2})\right\}, \tag{11}$$

- and

$$\lim_{r\to\infty}\{R, R^2, K\} \to 0. \tag{12}$$

Rotating solution

- We use solution generating technique "Newman-Janis" procedure

$$ds^2 = -f dt^2 + f^{-1} dr^2 + h d\Omega^2$$

Static "seed" metric

$$du = dt - dr/f$$

$$ds^2 = -f\, du^2 - 2\, du dr + h d\Omega^2$$

Null coordinate

$$g^{\mu\nu} = l^\mu n^\nu + l^\nu n^\mu - m^\mu \bar{m}^\nu - m^\nu \bar{m}^\mu$$

Define a null tetrad

$$l_\mu n^\mu = -m_\mu \bar{m}^\mu = 1 \quad otherwise\ 0$$

$$r' = r + ia\cos\theta \qquad u' = u - ia\cos\theta$$

$$l'^\mu = \delta^\mu_r, \quad n'^\mu = \delta^\mu_u - \frac{f(r')}{2} \delta^\mu_r$$

$$m'^\mu = \frac{1}{\sqrt{2h(r')}} \left(ia\sin\theta \left(\delta^\mu_u - \delta^\mu_r\right) + \delta^\mu_\theta + \frac{i}{\sin\theta} \delta^\mu_\phi \right)$$

$l'^\mu, n'^\mu, m'^\mu, \bar{m}'^\mu$

New null tetrad forms a new metric

$$du = dt - \frac{r^2 + a^2}{\Delta} dr, d\phi = d\phi' - \frac{a}{\Delta} dr$$

Transform a new metric to Boyer-Lindquist form

Rotating solution

- We obtain Kerr-like solution in the Boyer-Linquist coordinates

$$ds^2 = -\left(1 - \frac{\xi(r)}{\rho^2}\right) dt^2 + \frac{\rho^2}{\Delta} dr^2 + \rho^2 d\theta^2 - \frac{2\xi(r)}{\rho^2} a \sin^2\theta \, dt \, d\varphi \\ + \frac{\Sigma(r,\theta)}{\rho^2} \sin^2\theta \, d\varphi^2, \tag{13}$$

where

$$\xi(r) = r^2 (1 - f(r)), \tag{14}$$

$$\Delta(r) = r^2 + a^2 - \xi(r), \tag{15}$$

$$\Sigma(r,\theta) = (r^2 + a^2)^2 - \Delta a^2 \sin^2\theta. \tag{16}$$

- Smoothly reduce to static solution $f(r)$ ($a \to 0$), Kerr and Schwarzschild ($\rho_0 \to 0$).

Rotating solution

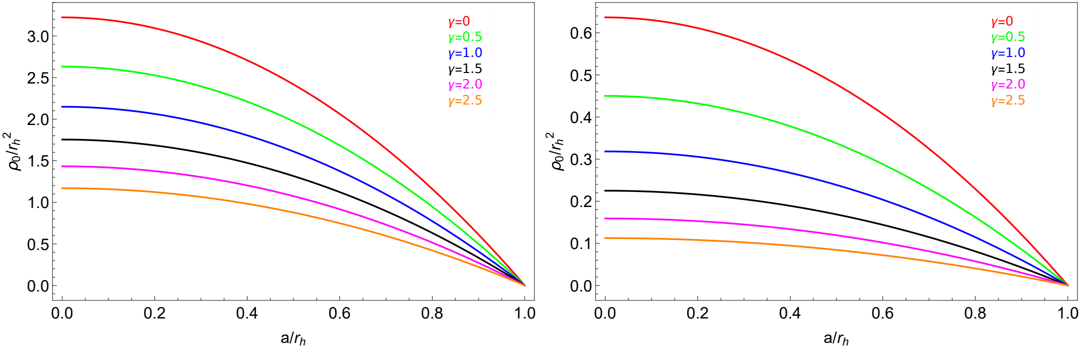

Figure: For fixed $r_0 = 0.5, 1.0$ (left, right)

Scalar pertubation

- We now consider a scalar field propagating in curved spacetime.

$$\frac{1}{\sqrt{-g}}\partial_\mu\left(\sqrt{-g}\,g^{\mu\nu}\partial_\nu\psi\right) - m^2\psi = 0, \tag{17}$$

- Substituting the following ansatz,

$$\psi(t, r, \theta, \phi) = e^{-i\omega t + i m_\ell \phi} R(r)\,\Theta(\theta). \tag{18}$$

Scalar pertubation

- We now consider a scalar field propagating in curved spacetime.

$$\frac{1}{\sqrt{-g}}\partial_\mu\left(\sqrt{-g}\,g^{\mu\nu}\partial_\nu\psi\right)-m^2\psi=0, \tag{17}$$

- Substituting the following ansatz,

$$\psi(t,r,\theta,\phi)=e^{-i\omega t+im_\ell\phi}R(r)\,\Theta(\theta). \tag{18}$$

- The angular equation is the spheroidal harmonics

$$\frac{1}{\sin\theta}\frac{d}{d\theta}\left(\sin\theta\frac{d\Theta}{d\theta}\right)+\left[a^2(\omega^2-m^2)\cos^2\theta-\frac{m_\ell^2}{\sin^2\theta}+\lambda_\ell^{m_\ell}\right]\Theta=0. \tag{19}$$

- The radial equation is obtained as

$$\frac{d}{dr}\left(\Delta\frac{dR}{dr}\right)+\left[\frac{\left((r^2+a^2)\omega-am_\ell\right)^2}{\Delta}-m^2r^2-a^2\omega^2+2am_\ell\omega-\lambda_\ell^{m_\ell}\right]R=0. \tag{20}$$

Quasinormal modes vs quasibound state

	QNMs	**QBS***
Field	massless/massive	massive ($m \neq 0$)
Horizon B.C.	ingoing: $e^{-i\omega r_*}$	ingoing: $e^{-i\omega r_*}$
Infinity B.C.	outgoing: $e^{+i\omega r_*}$	decaying: $e^{-\sqrt{m^2-\omega^2}\, r}$
$\mathrm{Re}(\omega)$	$\sim 1/M$	hydrogenic, $\approx m(1-(mM)^2/2n^2)$
$\mathrm{Im}(\omega)$	large (fast decay)	small for $mM \ll 1$
Picture	GW ringdown	gravitational atom[6]

[6] field bound in BH's potential well

- In this work, we shall work with the following assumptions

$$mM \ll 1, \qquad ma \ll 1, \qquad \omega a \ll 1. \tag{21}$$

- With these assumption, we can approximated

$$\lambda_\ell^{m_\ell} \approx \ell(\ell+1), \qquad \ell = 0, 1, 2, \ldots \tag{22}$$

- Here we consider only the Dehnen type profile $(1, 4, \gamma)$. The QBS will be obtained analytically via *asymptotic matching method*.

$$\frac{d}{dr}\left(\Delta\frac{dR}{dr}\right)+\left[\frac{\left((r^2+a^2)\omega-am_\ell\right)^2}{\Delta}-m^2r^2-a^2\omega^2+2am_\ell\omega-\lambda_\ell^{m_\ell}\right]R=0.$$

$(r \to \infty)$

$$\frac{d^2}{dx^2}(xR)+\left[-\frac{1}{4}+\frac{\nu}{x}-\frac{\ell(\ell+1)}{x^2}\right]xR=0.$$

$$A=-r_s-\frac{8\pi\rho_0r_0^3}{3-\gamma}$$

$$k^2\equiv m^2-\omega^2,\qquad \nu\equiv-\frac{Am^2}{2k},\qquad x\equiv 2kr,$$

$R_\infty \propto F_1(\ell+1-\nu, 2\ell+2, x)$

Confluent hypergeometric function

$(r \to r_h)$

$$z(z+1)Y''+(1+2iP+2z)Y'-\lambda_\ell^{m_\ell}Y=0.$$

$$P=-\frac{\omega\xi(r_h)-am_\ell}{2\kappa}.$$

$$\kappa\equiv r_h-\frac{1}{2}\xi'(r_h).\qquad z=\frac{r-r_h}{2\kappa},$$

$R_{r_h} \propto F_2(-\ell, \ell+1, 1+2iP, -z)$

hypergeometric function

Matching solutions in intermediate region

QBS frequency

The frequency

$$\omega \approx m\left(1-\frac{A^2m^2}{8n^2}\right) - 2i\frac{A^2m^3}{4n^3}\left[\frac{m\xi(r_h)-am_\ell}{2\kappa}\right]\left(\frac{2|A|\kappa m^2}{n}\right)^{2\ell+1}\times$$
$$\frac{(2\ell+1+n_r)!}{n_r!}\left[\frac{\ell!}{(2\ell)!(2\ell+1)!}\right]^2\prod_{j=1}^{\ell}\left(j^2+4P^2\right).$$

- $n_r \equiv -(\ell+1-\nu)$
- $m=0$, the frequency becomes trivial.

QBS frequency

The frequency

$$\omega \approx m\left(1-\frac{A^2m^2}{8n^2}\right) - 2i\frac{A^2m^3}{4n^3}\left[\frac{m\xi(r_h)-am_\ell}{2\kappa}\right]\left(\frac{2|A|\kappa m^2}{n}\right)^{2\ell+1}\times$$
$$\frac{(2\ell+1+n_r)!}{n_r!}\left[\frac{\ell!}{(2\ell)!(2\ell+1)!}\right]^2\prod_{j=1}^{\ell}\left(j^2+4P^2\right).$$

- $n_r \equiv -(\ell+1-\nu)$
- $m=0$, the frequency becomes trivial.
- $\omega_I \propto P \propto -[m\xi(r_h)-am_\ell] > 0$ (exponentially growth) if

$$\omega_R < m < \frac{m_\ell a}{r_h^2+a^2}. \tag{23}$$

QBS frequency

The frequency

$$\omega \approx m\left(1-\frac{A^2m^2}{8n^2}\right) -2i\frac{A^2m^3}{4n^3}\left[\frac{m\xi(r_h)-am_\ell}{2\kappa}\right]\left(\frac{2|A|\kappa m^2}{n}\right)^{2\ell+1}\times \frac{(2\ell+1+n_r)!}{n_r!}\left[\frac{\ell!}{(2\ell)!(2\ell+1)!}\right]^2\prod_{j=1}^{\ell}\left(j^2+4P^2\right).$$

- $n_r \equiv -(\ell+1-\nu)$
- $m=0$, the frequency becomes trivial.
- $\omega_I \propto P \propto -[m\xi(r_h)-am_\ell] > 0$ (exponentially growth) if

$$\omega_R < m < \frac{m_\ell a}{r_h^2+a^2}. \tag{23}$$

- Superradiant instability.

Amplification factor

- For scattering process, boundary condition of a radial function is (with real frequecy ω)

$$R \sim \begin{cases} \mathcal{T} e^{-i\omega r_*}, & \text{as } r_* \to -\infty \\ \mathcal{I} e^{-i\omega r_*} + \mathcal{R} e^{i\omega r_*}, & \text{as } r_* \to \infty. \end{cases}, \tag{24}$$

- One may define amplification factor as

$$Z = \frac{|\mathcal{R}|^2}{|\mathcal{I}|^2} - 1, \tag{25}$$

- Typically, $Z < 0$ as $\frac{|\mathcal{R}|^2}{|\mathcal{I}|^2} < 1$. (Wave is partially absorbed by BH)

Amplification factor

- For scattering process, boundary condition of a radial function is (with real frequecy ω)

$$R \sim \begin{cases} \mathcal{T} e^{-i\omega r_*}, & \text{as } r_* \to -\infty \\ \mathcal{I} e^{-i\omega r_*} + \mathcal{R} e^{i\omega r_*}, & \text{as } r_* \to \infty. \end{cases}, \tag{24}$$

- One may define amplification factor as

$$Z = \frac{|\mathcal{R}|^2}{|\mathcal{I}|^2} - 1, \tag{25}$$

- Typically, $Z < 0$ as $\frac{|\mathcal{R}|^2}{|\mathcal{I}|^2} < 1$. (Wave is partially absorbed by BH)

Amplification factor

- When superradiant condition is satisfied, it is possible that $Z > 0$, $\frac{|\mathcal{R}|^2}{|\mathcal{I}|^2} > 1$.
(Reflected wave come back bigger than the incident)

Amplification factor

- When superradiant condition is satisfied, it is possible that $Z > 0$, $\frac{|\mathcal{R}|^2}{|\mathcal{I}|^2} > 1$.
  (Reflected wave come back bigger than the incident)
- Here, we use (again) AMM to derive Z analytically.

Amplification factor

- When superradiant condition is satisfied, it is possible that $Z > 0$, $\frac{|\mathcal{R}|^2}{|\mathcal{I}|^2} > 1$. (Reflected wave come back bigger than the incident)
- Here, we use (again) AMM to derive Z analytically.

The factor

$$Z = \left| \frac{\left[\frac{\Gamma(2\ell+2)}{\Gamma(\ell+1-i\Lambda)} + \frac{\Gamma(-2\ell)}{\Gamma(-\ell-i\Lambda)}\left(\frac{B_2}{B_1}\right)\right](2iK)^{-i\Lambda-1}}{\left[(-1)^{-\ell-1+i\Lambda}\frac{\Gamma(2\ell+2)}{\Gamma(\ell+1+i\Lambda)} + (-1)^{\ell+i\Lambda}\frac{\Gamma(-2\ell)}{\Gamma(-\ell+i\Lambda)}\left(\frac{B_2}{B_1}\right)\right](2iK)^{-1+i\Lambda}} \right|^2 - 1,$$

$$\frac{B_2}{B_1} = \frac{\Gamma(\ell+1)\Gamma(-2\ell-1)\Gamma(\ell+1+2iP)}{\Gamma(2\ell+1)\Gamma(-\ell)\Gamma(2iP-\ell)}(4i\kappa K)^{2\ell+1},$$

$$K^2 = \omega^2 - m^2,$$

$$\Lambda = \frac{Am^2}{2K}.$$

Z vs ω

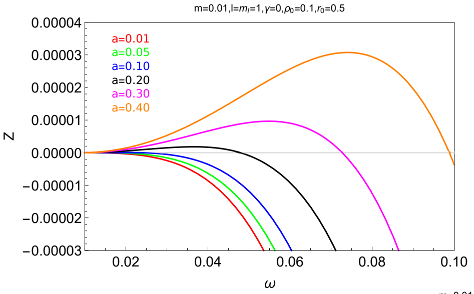
m=0.01,l=m_l=1,γ=0,ρ_0=0.1,r_0=0.5
a=0.01
a=0.05
a=0.10
a=0.20
a=0.30
a=0.40
Z
ω

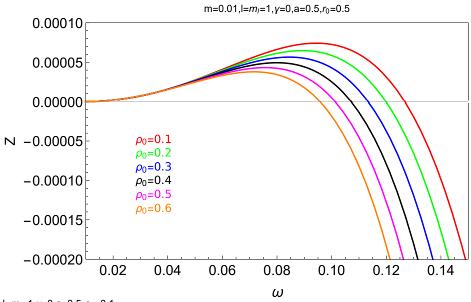
m=0.01,l=m_l=1,γ=0,a=0.5,r_0=0.5
ρ_0=0.1
ρ_0=0.2
ρ_0=0.3
ρ_0=0.4
ρ_0=0.5
ρ_0=0.6
Z
ω

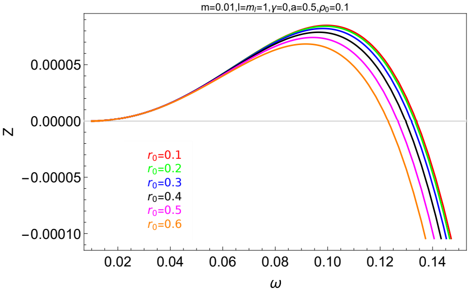
m=0.01,l=m_l=1,γ=0,a=0.5,ρ_0=0.1
r_0=0.1
r_0=0.2
r_0=0.3
r_0=0.4
r_0=0.5
r_0=0.6
Z
ω

Conclusions

- We construct static and rotating black holes with double power law dark matter profile.
- Quasibound state frequency and amplification factor are derived analytically via asymptotic matching method.
- Superradiant instability is found.

What's left to be done?

- black hole perturbation
- shadow
- particle motion
- end point of instability

Thank you